

Development of Fabrication of Giant Nanomembranes

Hirohmi Watanabe, Richard Vendamme, and Toyoki Kunitake*

Spatio-Temporal Function Materials Research Group, Frontier Research System (FRS),
The Institute of Physical and Chemical Research (RIKEN), 2-1 Hirosawa, Wako 351-0198

Received December 13, 2006; E-mail: kunitake@ruby.ocn.ne.jp

Large nanomembranes, which are characterized by aspect ratios (size/thickness) of greater than one million, are described. The combination of nanometer thickness and macroscopic size facilitates important applications in materials separation, selective transport and electrochemical devices. In the past, only small pieces of nanomembranes have been fabricated, in spite of intensive research. We describe here the first examples of a general fabrication procedure. Spin coating of the precursor solutions on appropriate underlayer was effectively used to prepare 10–30 nm thick nanomembranes of metal oxides, interpenetrating network of cross-linked acrylate with metal oxide, and highly cross-linked organic polymers (epoxy resin, etc.). The underlayer is composed of an affinity (e.g., poly(vinyl alcohol)) layer and/or sacrificial layer, and the role of these layers is discussed. Some of the mechanical properties of nanomembranes were measured by using a bulge test and a compression method. The nanomembranes of the organic and inorganic hybrids and the purely organic resins were surprisingly robust and defect-free.

1. Introduction

The science and technology of membranes has attracted much attention for many decades. Fundamental features that are desired for membrane function are defect-free uniformness, macroscopic robustness, high permeability, and tailor-made selectivity.[1] Such often conflicting properties should be achieved in an ultimate form, if nanometer-thick membranes with macroscopic mechanical stability and permeant-specific nanochannels are prepared. Ion channels and other transport systems in the biological membrane are ideal in this respect. Polymeric materials and inorganic materials have been used most frequently to fabricate practical separation membranes, but their thicknesses basically remained in the micrometer range. Development of nanometer-thick, free-standing membranes has been accelerated over the last decade.

In this review, we discuss our very recent results on fabrication of large nanomembranes. We define here "large nanomembrane" as having the following three features. First, its thickness is in the range of 1–100 nm. The self-supporting (free-standing) property is the second feature that is required for a membrane to be able to physically separate two spaces. Thirdly, the "large" nanomembrane should be characterized by an aspect ratio of size and thickness greater than 10^6, that is, if the membrane thickness is 10 nm, its size must be greater than 1 cm × 1 cm. Two related structural features are involved in these requirements. One is macroscopic mechanical strength (robustness), and the other is the uniform and defect-free nature over a large area. These specific targets will alleviate confusions in development of nanomembranes.

Prior to discussion of our results, it is appropriate to summarize recent efforts to prepare nanomembranes by other groups.

2. Nanometer-Thick Membranes from Linear Polymers and by the Langmuir–Blodgett (LB) Approach

Physical properties arising from extreme thinness of polymer membranes are a target of intensive research by polymer physicists due to possible quasi-2-dimensional behavior of polymer chain. As a typical example, Forrest et al. have prepared a free-standing films of polystyrene with a thickness of 29–184 nm by spin coating and have measured their glass-transition temperatures as a function of the film thickness to examine chain confinement effects in two dimensions. In this experiment, a 1 cm^2 piece has been transferred from water surface onto a 3 mm hole.[2] Nardin et al. have reported a 10 nm thick, self-supporting (1 mm^2 size) film by cross-linking of a black film of an ABA triblock copolymer.[3] Cross-linked elastomeric membrane of 40 nm thickness is obtained by LB transfer from water surface onto a copper grid with 70 μm hole without rupture.[4,5] A free-standing film of Nylon 13,13 has been prepared with thickness of 50 nm by casting its solution onto water, though it shrinks when removed from the water surface.[6] Quasi-2D objects of 5–30 nm thickness and 2 μm size have been fabricated from patterned, cross-linked polymer brushes.[7]

Kunitake et al. have reported the fabrication of two-dimensional cross-linked polysiloxane LB films.[8] The monolayer of an amphiphilic siloxane copolymer is cross-linked with poly(vinyl sulfate) and is transferred onto a solid substrate by the conventional LB technique. Most recently, Miyashita and co-

Published on the web March 13, 2007; doi:10.1246/bcsj.80.433

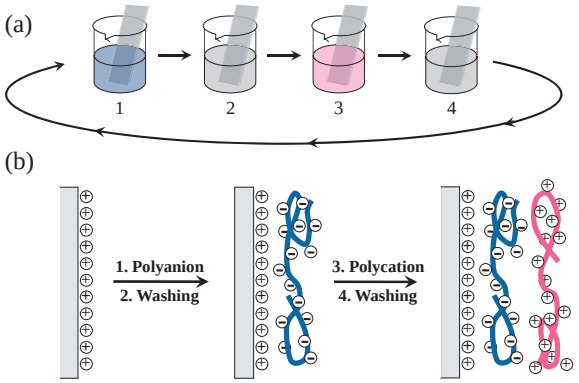

Fig. 1. (a) Schematic representation of the electrostatic alternative assembly process, and (b) the simplified molecular picture of the first cycle; steps 1 and 3 represent the adsorption process of polycation and polyanion, respectively, and steps 2 and 4 are washing steps. The drawing is adapted from Ref. 12.

workers have prepared LB multilayers of poly(*N*-dodecylacrylamide) copolymer, and have demonstrated that these nanosheets with sub-millimeter sizes are free-standing.[9]

3. Nanomembrane Formation by Layer-by-Layer Assembly

Other novel approaches are also being developed for molecularly thin layers. Most important is the electrostatic layer-by-layer assembly.[10–14] A schematic representation of the layer-by-layer procedure is shown in Fig. 1. This method is now widely used for the lamination of oppositely charged polymers, polymers with proteins, and organic with inorganic compounds in the molecular thickness. Preparation of the layer-by-layer assembled ultrathin hollow polymer shells (or nanotubes) has been extensively investigated by Caruso et al.[15–19] and by other groups.[20–26] The preparation of free-standing ultrathin films by this approach has been studied by several groups. Onda et al. have prepared enzyme-containing alternate films on porous filter membranes and examined sequential enzyme catalysis.[27] Huck et al. have isolated a free-standing hexagonal sheet (10 μm size and 5 nm thick) of alternate polyions.[28] Mamedov and Kotov have prepared free-standing ultrathin films that incorporate magnetite nanoparticles by dissolving away a cellulose acetate support on glass substrate.[29] Tsukruk and co-workers have discussed the mechanical properties of free-standing nanomembrane composites.[30–35] Very recently, Ono and Decher have obtained a free-standing polyelectrolyte multilayer with a few centimeter square size by using a suitable sacrificial layer.[36] The thickness of this film is estimated roughly to be 250 nm from the reported number of the deposition cycle. Unfortunately, these LbL methods could give nanofilms (thickness 30–70 nm) with few tens to few hundreds of nanometers, as summarized by Jiang and Tsukruk.[34]

4. Giant Nanomembranes of Metal Oxides

It is clear from the above examples that free-standing, nanometer-thick membranes have been obtained only as small pieces of membranes. It is not easy to impart to a single membrane both of macroscopic size and nanometer thickness.

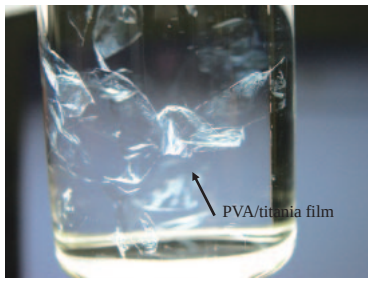

Fig. 2. A PVA/titania film in ethanol. The vial diameter is 27 mm.

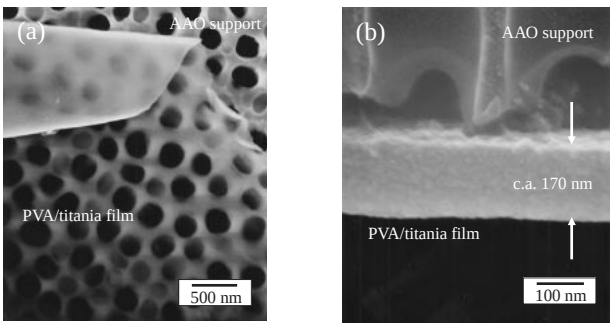

Fig. 3. SEM images of a PVA/titania film on an anodized aluminum oxide (AAO) support; (a) top view, and (b) cross-section view.

There are, to the best of our knowledge, no previous examples where centimeter size is combined with sub-100 nm thickness.

We studied a novel fabrication procedure of metal oxide nanolayers by sequential sol–gel process.[37,38] A similar procedure has been independently reported by Kleinfeld and Ferguson.[39] We attempted to apply this approach to the preparation of self-supporting metal oxide nanofilms.[40] For example, a composite (polymer/metal oxide) thin layer was prepared on a sacrificial polymer underlayer and then detached from the substrate by dissolving the polymer layer alone. Unfortunately, the size of the obtained ultrathin (polymer/metal oxide) composite film with thickness of ca. 20 nm could not be made larger than approximately 15 mm^2. The original film fragmented readily upon dispersion in solvents.

These problems were solved by a new approach that included the use of designed "double layer" and spin-coating techniques.[41] Photoresist polymers can be used as sacrificial underlayers, since some of them are highly soluble in ethanol and can be uniformly spin-coated onto a silicon wafer. On the other hand, a poly(vinyl alcohol) (PVA) layer provides a homogeneous surface rich in hydroxy groups, and it promotes the hydrolysis of metal alkoxide to form metal oxide layer homogeneously. Thus, an ultrathin titania layer was formed from titanium butoxide by spin-coating onto a double layer of PVA/photoresist layer on Si wafer. This specimen was placed in a Petri dish, and ethanol was added to remove the photoresist layer, leaving behind a free-standing ultrathin PVA/titania film. It is transparent, uniform and flexible (Fig. 2). The corresponding SEM observation indicates that the membrane (3 × 4 cm) on an anodized aluminum oxide (AAO) disk is uniform and defect-free with a thickness of 140 nm (Fig. 3). Much thinner membranes were possible when dilute precursor solutions

Table 1. Self-Supporting PVA/Metal Oxide Nanofilms

Sample no.	Film composition[a)]	Film thickness/nm[b)]
1	PVA/TiO_2[c)]	140 ± 25
2	PVA/TiO_2[c),d)]	13 ± 1.2
3	PVA/Al_2O_3	57 ± 17
4	PVA/NbO_5	54 ± 5.5
5	PVA/ZrO_2	50 ± 8.4
6	PVA/SiO_2	17 ± 1.9
7	PVA/La_2O_3[e)]	nd
8	PVA/(4-PABA + TiO_2)[c),f)]	190 ± 32
9	PVA/(4-PABA + Al_2O_3)[g)]	46 ± 15
10	$(PVA/TiO_2)_3$	89 ± 7.3

a) [Metal alkoxide]: 100 mM in the spin-coating solution (solvent; $CHCl_3$). The photoresist polymer was used as sacrificial layer. b) Mean ± SD, nd: not determined. c) From Ref. 19. d) [$Ti(OBu_4)$]: 10 mM. e) The spin-coating solution was suspended and powders were deposited on the film surface. f) [(4-Phenylazo)benzoic acid]: 20 mM. g) [(4-Phenylazo)-benzoic acid]: 10 mM.

were employed, and a free-standing membrane with thickness of 13 nm was obtained. As far as we know, this is the thinnest self-supporting membrane that can maintain its size as large as 10 cm^2 for several months at least. The major advantage of this approach over the previous surface sol–gel method is 2-fold. First, spin coating appears to give a more uniform layer over a large area than the chemical adsorption step in the former, though monolayer adsorption is not assured. The second is the use of a "double layer," in which the photoresist (TDUR-P015, Tokyo Ohka) layer facilitates membrane detachment and the PVA layer promotes 2-dimensional networking of nascent titania layer.

Subsequently, the spin-coating approach was extended to other metal oxide membranes.[42] Spin coating of various metal oxide precursors was performed on the double underlayer-coated Si wafer. Table 1 summarizes some of the results. In all cases, self-supporting ultrathin films were obtained. Film thickness determined by SEM observation was strongly dependent on the kind of metal alkoxides, due to their different reactivity. The macroscopic and SEM pictures of these films were very similar to those of the PVA/titania film.

Conventional ceramic films have high network density and are commonly considered as hard materials. However, metal oxide nanofilms fabricated as described above were significantly soft (flexible), and were totally different from thicker ceramic films. The softness of these nanofilms was attributed to their amorphous, disordered, and ultrathin characters.[43]

The structural adaptability of bonding network of metal oxides is exemplified by nanocopying and molecular imprinting. We define nanocopying as the "copying of nanometer-sized objects, such as molecules, supramolecules, nanoparticles, and surface morphologies, with nanometer precision."[44] Materials that can be employed for this purpose must be uniform, shape-adaptable with nanometer precision, and self-supporting. The combination of chemical inertness and physical softness allows further applications to biomaterials. Our recent studies showed that biomolecules (proteins) readily assembled on a variety of substrates modified with titania nanofilms, and retained their biological activities.[45] It was also possible to embed individual ferritin molecules, a large globular protein, in a large silica nanofilm with 15 nm thickness.[46]

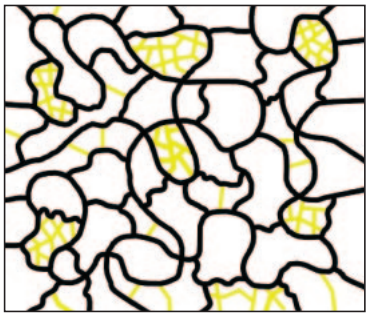

Fig. 4. Schematic illustration of the interpenetrated network of organic (in black) and inorganic (in yellow) components.

5. Nanomembrane of Organic and Inorganic Hybrids[47,48]

The spin-coating process is effective for the preparation of macroscopically uniform, self-supporting metal oxide gel films with thickness of several tens of nanometers and lateral dimensions of several centimeters. Unfortunately, the stiff inorganic network can easily cause damage to the film soon after dissolution of the sacrificial layer, probably due to local concentration of applied stress. This must be overcome to make the film robust enough. Organic and inorganic hybrid materials with interpenetrating network structures combine advantages of organic polymers (versatility, flexibility, and light weight) and the physical property of inorganic glasses (heat and mechanical resistance). This unique combination is effective for providing robust, free-standing nanomembranes. The fabrication procedure is rather simple. In the first example, the inorganic precursor was zirconium tetrabutoxide, and the organic precursor was a combination of mono-functional monomer (4-hydroxybutyl acrylate), bifunctional cross-linking agent (hexanediyl diacrylate), and photo-initiator (Darocure 4265). Simultaneous polymerization and polycondensation during the spin-coating process gave nanomembranes with an interpenetrated network of the two components, as schematically shown in Fig. 4. A top-view SEM image of the resulting nanomembrane on an AAO support (Figs. 5a and 5b) showed the formation of a uniform 35 nm thick layer without defects and cracks. From TEM observations (Fig. 5c), a smooth, amorphous surface is formed with the lowest zirconium dioxide (ZrO_2) fractions, but regular lattices with domain sizes of 5 to 10 nm is observed when the ZrO_2 content was increased (Fig. 5d).

The self-supporting nanomembrane floating in ethanol (Fig. 6a) was very flexible, robust, and could be easily folded into small shapes. Figure 6b shows camera views of the aspiration process of a 16 cm^2 nanomembrane into a micropipette with a tip diameter of approximately 320 μm. The membrane could pass completely through a micropipette with 30000 times smaller hole, due to its extreme thinness and flexibility, and could be again released into the solvent without breaking. Soon after releasing, the hybrid ultrathin membrane adopted a folded morphology but rapidly regained its original film shape by gentle manipulation with a spatula. The ability of the nanomembrane to "flow" into such tiny orifices is an indication of its extreme flexibility. Such experiments could not be per-

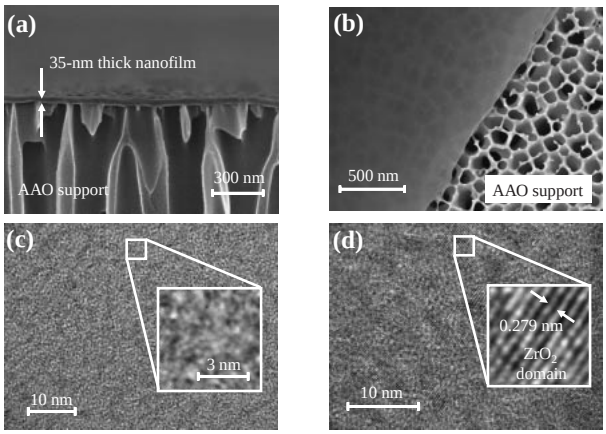

Fig. 5. Microscopic characterization of free-standing hybrid nanofilms. (a) SEM side-view image of a nanomembrane on AAO support. (b) SEM top-view image of a nanomembrane. (c) TEM image of a low-ZrO_2 nanomembrane on a copper grid. (d) TEM image of a high-ZrO_2 nanomembrane showing the presence of an ordered domain dispersed in an amorphous matrix.

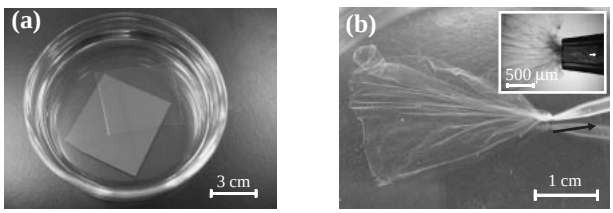

Fig. 6. (a) An IPN hybrid nanofilm detached from the substrate and floating in ethanol, and (b) the aspiration process of a 16 cm^2 nanofilm into a micropipette with a tip diameter of 320 μm (inset; close-up micrograph around the tip during the aspiration process).

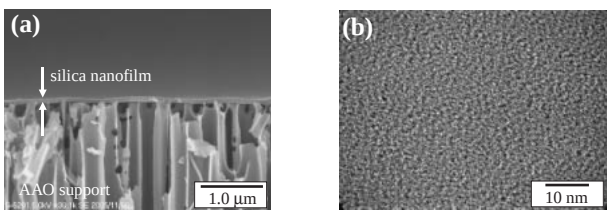

Fig. 7. (a) SEM side-view image of a SiO_2/polymer hybrid nanomembrane on AAO support. (b) TEM image of a SiO_2/polymer hybrid nanomembrane on a copper grid.

formed for the pure inorganic films because the film was easily damaged.

Essentially, the same results were obtained when the zirconia component was replaced with silica. The SEM top view of Fig. 7a shows that the pores of ANODISC (pore size, 200 nm and smaller) are fully covered with the nanofilm without any defects or cracks. TEM observation was performed on IPN nanofilms that were transferred onto a Cu grid (Fig. 7b). A smooth amorphous surface formed, and the organic and inorganic components were both amorphous and appeared to be molecularly uniform with an SiO_2 content of around 35 mol %. This is contrasting with the presence of a regular zirconia lattice at a similar content.

Table 2. Mechanical Properties of IPN Hybrid Nanofilms

Sample no.	MO_x content /mol %[a)]	Young's modulus /Pa[b)]	Ultimate tensile stress /Pa[c)]	Ultimate elongation /%[c)]
Silica-1	21.9	1.3×10^8	7.3×10^7	4.9
Silica-2	26.2	6.9×10^8	6.5×10^7	2.1
Silica-3	34.5	1.1×10^9	4.5×10^7	1.3
Zirconia-1	11.2	3.5×10^8	1.1×10^8	2.6
Zirconia-2	17.8	4.0×10^8	6.8×10^7	1.4
Zirconia-3	22.5	nd[d)]	nd[d)]	nd[d)]

a) Determined by XPS measurements. b) Determined by "strain-induced elastic buckling instability for mechanical measurements (SIEBIMM)." c) Determined by bulging experiments. d) Fragmented into small pieces.

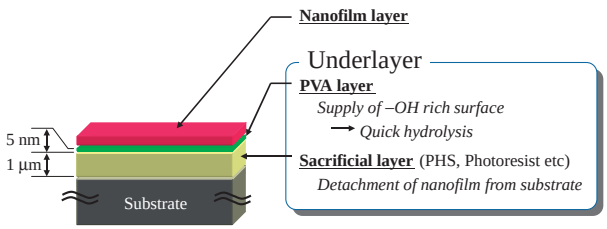

Fig. 8. Multilayer structure in the fabrication of nanomembrane.

The mechanical property of the IPN hybrids is summarized in Table 2. Decrease in the metal oxide content resulted in a significantly lower elastic modulus. The nanomembranes reinforced with zirconia had substantially higher moduli than those of silica hybrids. From a bulge test, the ultimate tensile stress (σ) and ultimate elongation (ε) were suppressed with an increase in the silica. The silica hybrid with a lower silica content (22 mol % for Silica-1) shows a lower modulus but is more "robust" in the free-standing state. Their greater elasticity apparently dissipates the fracture energy and prevents crack developments.

6. Some Features Unique to Nanomembrane Fabrication

In the course of the nanomembrane study, several new techniques that are indispensable for the fabrication process were employed. They are the development of proper underlayer on one hand, and the use of newer methods for determination of mechanical properties.

6.1 The Importance of Underlayer. A schematic illustration of a typical underlayer is shown in Fig. 8. The underlayer can be composed of the double layer of a PVA upperlayer and a sacrificial layer. This is not the case in the fabrication of pure organic nanomembranes, because sacrificial layer alone is sufficient. In any case, the presence of sacrificial layer is essential in fabrication of free-standing nanomembranes, since nanomembranes directly formed on common solid substrates cannot be detached as such because of their ultrathin nature. On the other hand, ultrathin PVA layer was particularly effective for reproducible preparation of uniform, free-standing ceramic membranes by spin coating. Apparently, the PVA layer provides a homogeneous surface rich in the hydroxy group, and this enhances the networking of the metal oxide units along the surface. Other polymers, which have hydroxy or carboxy groups, may also be useful for this purpose. When poly(acrylic

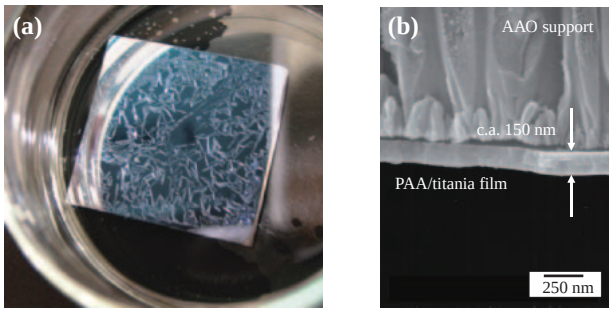

Fig. 9. (a) A PAA/titania film in ethanol, and (b) SEM image of the piece of the PAA/titania film.

acid) (PAA) was used as the sole underlayer, the resultant ceramic film fragmented into small pieces immediately (Fig. 9a). However, the SEM image indicated the existence of a uniform film morphology (Fig. 9b) similar to the case of PVA underlayer. In the case of dextran underlayer, an ultrathin film was obtained, however, the size was much smaller than that of the original substrate, and the film surface was not homogeneous.

The role of sacrificial underlayer is to facilitate detachment of membranes from solid substrates. Photoresist TDUR-P015 (Tokyo Ohka, Co.), which is phenolic resin for KrF lithography, is quite suitable as sacrificial layer, because the resin is highly soluble in ethanol. Poly(*p*-hydroxystyrene) (PHS) is also useful as sacrificial layer. When PHS was spin-coated on Si wafer, followed by the formation of PVA/TiO_2 double layer, a free-standing PVA/TiO_2 membrane could be readily detached in ethanol. These sacrificial layers can be applied to fabrication of inorganic membrane as well as of organic membrane. However, solvents employed for dissolution are more varied in the latter case, and it is necessary to develop a sacrificial layer that may be used more generally, since different solvents are used for different membrane precursors. The sacrificial underlayer must remain intact against various solvents employed during the spin-coating process, and additionally, it should be readily dissolved in common organic solvents during the film detachment process. These two conflicting properties are required for a general-purpose sacrificial underlayer.

This problem was solved by the use of "thermally crosslinkable and photo-decomposable" polymer mix.[49] The polymer mix was composed of a hydroxy polymer, a divinyl ether, and a photo-acid generator (PAG). As shown in Fig. 10, thermal reaction of hydroxy-bearing polymer with divinyl ether gave an insoluble, infusible cross-linked material. The cross-linked structure, however, decomposed by acid-catalyzed thermal reaction. Thus, photo-generated acid from PAG, and additional baking converts the insoluble layer to readily soluble products.

6.2 Mechanical Measurement of Nanomembrane. What is the basic mechanical property required for large, robust nanomembranes? The robustness may be guaranteed by the lack of weak points, a reasonable magnitude of tensile strength and the absence of plastic deformation. Stress concentration that leads to destruction may be avoided by defect-free homogeneity of the membrane matrix. Two important methodologies have been developed to determine such mechanical properties of nanomembranes.

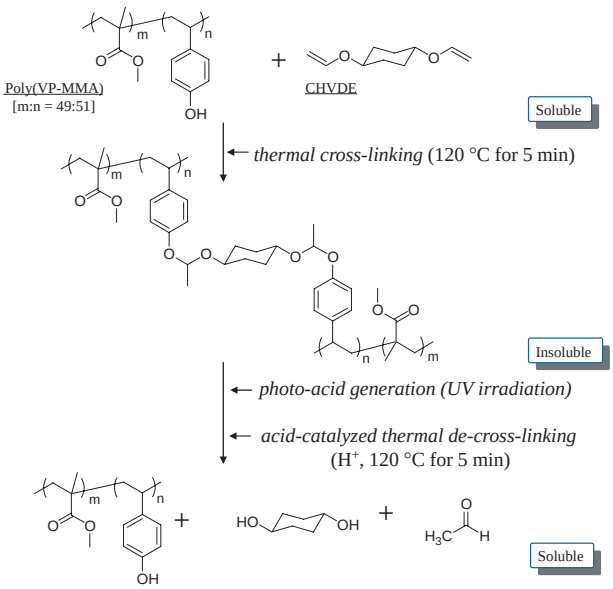

Fig. 10. Chemical reactions of "thermally crosslinkable and photo-decomposable" polymer mix during the preparation procedure. Acid is generated by photo-decomposition of PAG.

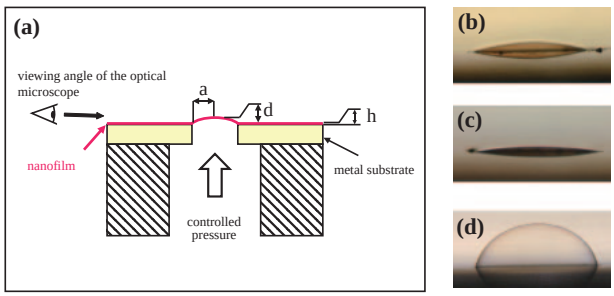

Fig. 11. Bulging experiment; (a) experimental setup, (b)–(d) lateral views of various deflected nanomembranes under overpressure.

6.2.1 Bulge Test: Measurement of Tensile Strength and Ultimate Elongation: Goedel and Heger have introduced the bulge test for measuring the mechanical properties of nanofilms.[50] The experimental setup is shown in Fig. 11a. The nanomembrane is attached on a metal plate with a circular hole, and air pressure is applied to the nanomembrane from backside through the hole. Applied overpressure is monitored by a digital manometer, and the deflection behavior of the membrane is observed with an optical microscope. Microscopic pictures in Figs. 11b–11d are examples of the deflected nanomembrane.

The values of σ and ε are determined using the following formula

$$\sigma = (P \times a^2)/(4 \times h \times d), \quad (1)$$

$$\varepsilon = (2 \times d^2)/(3 \times a^2), \quad (2)$$

where P is the pressure required to break the membrane, a is the radius of the metal hole (1 mm), h is the membrane thickness determined by SEM observation, and d is the deflection of the membrane at the rupture pressure.

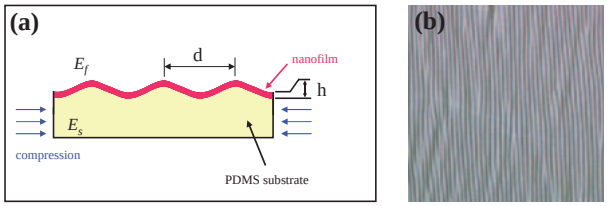

Fig. 12. SIEBIMM experiment; (a) Schematic illustration of strain-induced elastic buckling instability, and (b) microscopic picture of an obtained buckling texture of nanomembrane.

6.2.2 Measurement of Young's Modulus: Young's modulus is estimated by the "strain-induced elastic buckling instability for mechanical measurements (SIEBIMM)" technique. Strain-induced elastic buckling instability has been reported to make an ordered structure,[51] and the phenomena has been widely used for the determination of mechanical properties of nanofilms.[52] This technique utilizes buckling instability that occurs in a bi-layer consisting of a stiff, thin layer and a relatively soft, thick substrate layer (polydimethylsiloxane; PDMS employed most often) as shown in Fig. 12a. Upon applying compression, the bi-layer produces highly periodic wrinkles, and the elastic modulus can be calculated from the pitch of the periodic buckling wavelength (Fig. 12b). In practice, the PDMS composite is compressed by a small vise, and the periodic wavelength of the wrinkle is monitored by an optical microscope and AFM. Young's modulus is determined using the following formulae

$$E_f = 3E_s \times (1 - \nu_f^2)/(1 - \nu_s^2) \times (d/2\pi h)^3, \quad (3)$$

where E_s is the Young's modulus of PDMS, ν_f and ν_s are the Poisson's ratio of nanofilm and substrate, respectively, and h is the nanofilm thickness.

7. Totally Organic Nanomembranes

Fabrication of robust free-standing membrane is not limited to ceramic components and organic/inorganic hybrids. In general, hard materials, even if highly cross-linked, become soft when their sizes, thickness in particular, are reduced to the nanometer regime. Thermosetting resins are a representative class of the hard material, being insoluble and infusible upon cross-linking by thermal treatment. Epoxy resin is a favorite choice, since this resin has superior adhesiveness, dimensional stability, chemical resistance and electrical inertness. We fabricated epoxy nanomembrane by spin-coating procedure using PHS as sacrificial layer.[53] The detached film maintained the size of the spin-coated area. A large, flexible film with a size of over 5 cm^2 was obtained even when the film thickness was as small as 20 nm (Fig. 13a). The cross sectional view of the nanomembrane after transfer onto AAO support is given in Fig. 13b. A uniform thickness of 23 $\pm$ 2 nm was obtained as the thinnest, free-standing nanomembrane without any signs of cracks and other defects on the membrane surface.

It is important to determine if the outstanding properties of the organic resin are retained even at the nanometer thickness. Some of the mechanical properties were measured by bulge test and SIEBIMM technique. The value of σ for the thinnest epoxy membrane was determined to be 30 MPa, which is within the range of those for the conventional thick epoxy resins of different compositions (1–100 MPa). The electrical properties were studied by measuring the output leakage current on a potentiostat/galvanostat system. The nanomembrane was transferred onto the surface of p-type silicon wafer, and platinum electrodes (1 mmφ) were evaporated onto the top through a shadow mask to form the metal–insulator–semiconductor (MIS) stack, Pt/nanomembrane/p-Si. The output leakage current of the epoxy membrane (30 nm thick) was about 90 µA at 0.5 V, and the electric resistivity was calculated as 0.5×10^{11} [Ω cm]. The high electric insulation was additional evidence for the defect-free nature of the nanomembrane. The conventional bisphenol A-type epoxy resin gives a similar range of electric resistivity of 10^{10}–10^{12} [Ω cm],[54] and therefore, the electrical properties remain essentially the same in the form of nanomembrane.

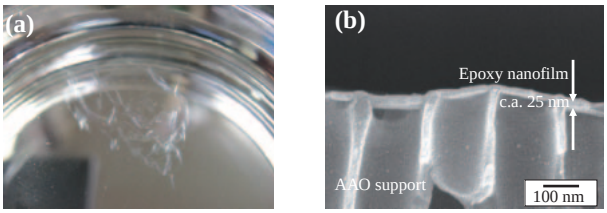

Fig. 13. (a) A epoxy nanomembrane in ethanol, and (b) SEM image of epoxy nanomembrane on AAO support.

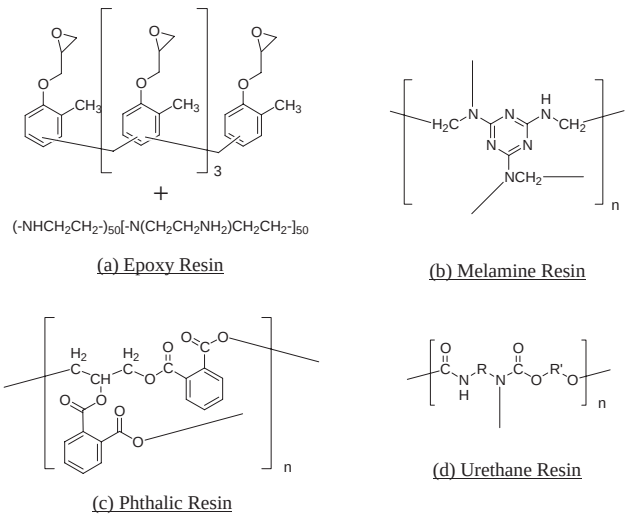

Fig. 14. Typical chemical structures of (a) epoxy resin, (b) melamine resin, (c) phthalic resin, and (d) urethane resin.

Similar organic nanomembranes were obtained from other cross-linked organic macromolecules, such as melamine resin, urethane resin, and phthalic resin.[49] Typical chemical structures of these resins are shown in Fig. 14. The physical properties of these nanomembranes appear to reflect those of the corresponding macroscopic resins. For example, the urethane nanomembrane showed plastic deformation unlike other nanomembranes, when air pressure was applied in the bulge test. Successful fabrication of nanomembranes from rich combinations of precursor materials is important for the functionalization of nanomembranes toward biomedical applications, designed transport of ions and molecules, and separation purposes.

8. Concluding Remarks

The nanomembranes as described above possess several novel features of nanomaterials. Nanomaterials may be classified as nanodots, nanowires, and nanolayers, depending on the number of nano-dimensions. A nanolayer is characterized as having only one nano-dimension; the other two dimensions are macroscopic. A nanomembrane is defined as being self-supporting, in addition to the intrinsic nanolayer properties. The nanometer thickness provides versatile possibilities for materials separation. Reverse osmosis and the electrolyte membrane in fuel cell are typical examples. Thicknesses close to those of biomembranes will also facilitate construction of molecular devices, in which individual molecules play vital roles. Design of novel molecular systems will become a reality.

References

1 M. Mulder, *Basic Principles of Membrane Technology*, 2nd ed., Kluwer Academic Publishers, Dordrecht, The Netherlands, **1996**.

2 J. A. Forrest, K. Dalnoki-Veress, J. R. Dutcher, *Phys. Rev. E* **1997**, *56*, 5705.

3 C. Nardin, M. Winterhalter, W. Meier, *Langmuir* **2000**, *16*, 7708.

4 F. Mallwitz, W. A. Goedel, *Angew. Chem., Int. Ed.* **2001**, *40*, 2645.

5 H. Xu, R. Heger, F. Mallwitz, M. Blankenhagel, C. Pevratout, W. A. Goedel, *Macromol. Symp.* **2002**, *177*, 175.

6 L. H. Wang, R. S. Porter, *J. Polym. Sci., Part B: Polym. Phys.* **1995**, *33*, 785.

7 S. Edmondson, W. T. S. Huck, *Adv. Mater.* **2004**, *16*, 1327.

8 M. Kunitake, T. Nishi, H. Yamamoto, K. Nasu, O. Manabe, N. Nakashima, *Langmuir* **1994**, *10*, 3207.

9 H. Endo, Y. Kado, M. Mitusishi, T. Miyashita, *Macromolecules* **2006**, *39*, 5559.

10 G. Decher, J.-D. Hong, *Ber. Bunsen-Ges. Phys. Chem.* **1991**, *95*, 1430.

11 G. Decher, J.-D. Hong, *Makromol. Chem., Macromol. Symp.* **1991**, *46*, 321.

12 G. Decher, *Science* **1997**, *277*, 1232.

13 G. Decher, in *Comprehensive Supramolecular Chemistry*, ed. by J. L. Atwood, J. E. D. Davies, D. D. Macnicol, F. Vögtle, J.-M. Lehn, Pergamon, Oxford, **1996**, Vol. 9, pp. 507–528.

14 P. Bertrand, A. Jonas, A. Laschewsky, R. Legras, *Macromol. Rapid Commun.* **2000**, *21*, 319.

15 F. Caruso, R. A. Caruso, H. Möhwald, *Science* **1998**, *282*, 1111.

16 F. Caruso, *Chem. Eur. J.* **2000**, *6*, 413.

17 F. Caruso, *Adv. Mater.* **2001**, *13*, 11.

18 E. Donath, G. B. Sukhorukov, F. Caruso, S. A. Davis, H. Möhwald, *Angew. Chem., Int. Ed.* **1998**, *37*, 2202.

19 M.-K. Park, C. Xia, R. C. Advincula, P. Schütz, F. Caruso, *Langmuir* **2001**, *17*, 7670.

20 S. M. Marinakos, D. A. Shultz, D. L. Feldheim, *Adv. Mater.* **1999**, *11*, 34.

21 S. M. Marinakos, J. P. Novak, L. C. Brousseau, III, A. B. House, E. M. Edeki, J. C. Feldhaus, D. L. Feldheim, *J. Am. Chem. Soc.* **1999**, *121*, 8518.

22 S. M. Marinakos, M. F. Anderson, J. A. Ryan, L. D. Martin, D. L. Feldheim, *J. Phys. Chem. B* **2001**, *105*, 8872.

23 J. Hotz, W. Meier, *Langmuir* **1998**, *14*, 1031.

24 B. M. Discher, Y.-Y. Won, D. S. Ege, J. C.-M. Lee, F. S. Bates, D. E. Discher, D. A. Hammer, *Science* **1999**, *284*, 1143.

25 T. Sanji, Y. Nakatsuka, S. Ohnishi, H. Sakurai, *Macromolecules* **2000**, *33*, 8524.

26 S. O. Obare, N. R. Jana, C. J. Murphy, *Nano Lett.* **2002**, *1*, 601.

27 M. Onda, Y. Lvov, K. Ariga, T. Kunitake, *J. Ferment. Bioeng.* **1996**, *82*, 502.

28 W. T. S. Huck, A. D. Stroock, G. M. Whitesides, *Angew. Chem., Int. Ed.* **2000**, *39*, 1058.

29 A. A. Mamedov, N. A. Kotov, *Langmuir* **2000**, *16*, 5530.

30 C. Jiang, S. Markutsya, V. V. Tsukruk, *Adv. Mater.* **2004**, *16*, 157.

31 S. Markutsya, C. Jiang, Y. Pikus, V. V. Tsukruk, *Adv. Funct. Mater.* **2005**, *15*, 771.

32 C. Jiang, V. V. Tsukruk, *Soft Matter* **2005**, *1*, 334.

33 C. Jiang, D. S. Kommireddy, V. V. Tsukruk, *Adv. Funct. Mater.* **2006**, *17*, 27.

34 C. Jiang, V. V. Tsukruk, *Adv. Mater.* **2006**, *18*, 829.

35 C. Jiang, S. Singamaneni, E. Merrick, V. V. Tsukruk, *Nano Lett.* **2006**, *6*, 2254.

36 S. S. Ono, G. Decher, *Nano Lett.* **2006**, *6*, 592.

37 I. Ichinose, H. Senzu, T. Kunitake, *Chem. Lett.* **1996**, 831.

38 I. Ichinose, H. Senzu, T. Kunitake, *Chem. Mater.* **1997**, *9*, 1296.

39 E. R. Kleinfeld, G. S. Ferguson, *Mater. Res. Soc. Symp. Proc.* **1994**, *351*, 419.

40 M. Hashizume, T. Kunitake, *RIKEN Rev.* **2001**, *38*, 36.

41 M. Hashizume, T. Kunitake, *Langmuir* **2003**, *19*, 10172.

42 M. Hashizume, T. Kunitake, *Soft Matter* **2006**, *2*, 135.

43 J. He, T. Kunitake, *Soft Matter* **2006**, *2*, 119.

44 T. Kunitake, S. Fujikawa, *Aust. J. Chem.* **2003**, *56*, 1001.

45 A. Ghanashyam, T. Kunitake, *Langmuir* **2003**, *19*, 2260.

46 S. Fujikawa, E. Muto, T. Kunitake, *Langmuir* **2007**, in press.

47 V. Richard, S. Onoue, A. Nakao, T. Kunitake, *Nat. Mater.* **2006**, *5*, 494.

48 R. Vendamme, T. Ohzono, A. Nakao, M. Shimomura, T. Kunitake, *Langmuir* **2007**, in press.

49 H. Watanabe, T. Ohzono, T. Kunitake, *Macromolecules* **2007**, in press.

50 W. A. Goedel, R. Heger, *Langmuir* **1998**, *14*, 3470.

51 N. Bowden, S. Brittain, A. G. Evans, J. W. Hutchinson, G. M. Whitesides, *Nature* **1998**, *393*, 146.

52 C. M. Stafford, C. Harrison, K. L. Beers, A. Karim, E. J. Amis, M. R. Vanlandingham, H.-C. Kim, W. Volksen, R. D. Miller, E. E. Simonyi, *Nat. Mater.* **2004**, *3*, 545.

53 H. Watanabe, T. Kunitake, *Adv. Mater.* **2007**, in press.

54 *Handbook of Epoxy Resins*, ed. by H. Lee, K. Neville, McGraw-Hill Handbook, New York, **1967**, Chap. 6.

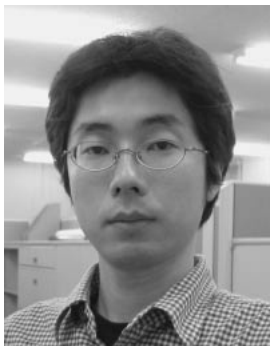

Hirohmi Watanabe was born in Aichi prefecture in 1974. He holds his B.E. (1997), M.E. (1999), and Ph.D. (2002) degrees from Chiba University. During his first year of the Ph.D. study, he was at the University of Massachusetts at Lowell as a visiting researcher, working under the supervision of Prof. Sukant Tripathy. After earning a Ph.D., he joined the Institute of Physical and Chemical Research (RIKEN). His current research interest is functional materials, especially for photofunctional materials.

Richard Vendamme was born in Bethune, France in 1978. After he obtained a master degree in organic and macromolecular chemistry from the University of Lille, he earned a doctor degree at the Max-Planck Institute for Polymer Research in Germany. He was subsequently awarded JSPS Postdoctoral Fellowship for Foreign Researchers enabling him to start research in Frontier Research System of RIKEN. His research interest include stimuli-responsive liquid crystalline gels and free-standing hybrid nanofilms.

Toyoki Kunitake was born in Kurume City, Japan, in 1936. He obtained B.Eng. and M.Eng. from Kyushu University, and subsequently earned a Ph.D. from the University of Pennsylvania. After postdoctoral research at the California Institute of Technology, he spent his career at Kyushu University until 1999. He served as Dean of Engineering at Kyushu and acted as principal investigator of the ERATO and ICORP projects (JST). He now heads the Spatio-Temporal Function Materials group at Frontier Research System of RIKEN and serves as vice president of University of Kitakyushu. His research interests involve physicochemical and organic aspects of synthetic bilayer membranes and molecular films, novel aspects of metal oxide nanofilms including molecular imprinting.